Exploratory Clinical Investigation of (4*S*)-4-(3-^{18}F-Fluoropropyl)-L-Glutamate PET of Inflammatory and Infectious Lesions

Sun Young Chae[1], Chang-Min Choi[2], Tae Sun Shim[2], Yangsoon Park[3], Chan-Sik Park[3], Hyo Sang Lee[1], Sang Ju Lee[1], Seung Jun Oh[1], Seog-Young Kim[4], Sora Baek[5], Norman Koglin[6], Andrew W. Stephens[6], Ludger M. Dinkelborg[6], and Dae Hyuk Moon[1]

[1]*Department of Nuclear Medicine, Asan Medical Center, University of Ulsan College of Medicine, Seoul, Republic of Korea;* [2]*Department of Pulmonology, Asan Medical Center, University of Ulsan College of Medicine, Seoul, Republic of Korea;* [3]*Department of Pathology, Asan Medical Center, University of Ulsan College of Medicine, Seoul, Republic of Korea;* [4]*Institute for Innovative Cancer Research, Asan Medical Center, University of Ulsan College of Medicine, Seoul, Republic of Korea;* [5]*Department of Nuclear Medicine, Kangdong Sacred Heart Hospital, Hallym University College of Medicine, Seoul, Republic of Korea; and* [6]*Piramal Imaging, Berlin, Germany*

We explored system x_C^- transporter activity and the detection of inflammatory or infectious lesions using (4*S*)-4-(3-^{18}F-fluoropropyl)-L-glutamate (^{18}F-FSPG) PET. **Methods:** In 10 patients with various inflammatory or infectious diseases, as many as 5 of the largest lesions were selected as reference lesions. ^{18}F-FSPG images were assessed visually and quantitatively. Expression levels of xCT, CD44, and surface markers of inflammatory cells were evaluated by immunohistochemistry. **Results:** ^{18}F-FSPG PET detected all reference lesions. ^{18}F-FSPG uptake in sarcoidosis was significantly higher than that in nonsarcoidosis. The lesion–to–blood-pool SUV ratio for ^{18}F-FSPG was comparable to that for ^{18}F-FDG in sarcoidosis. In nonsarcoidosis, however, it was significantly lower. In 5 patients with available tissue samples, the SUV_{max} for ^{18}F-FSPG and CD163 were negatively correlated ($\rho = -0.872$, $P = 0.054$). **Conclusion:** ^{18}F-FSPG PET may detect inflammatory lesions when activated macrophages or monocytes are present, such as in sarcoidosis.

Key Words: glutamate; x_C^- transporter; positron emission tomography; inflammation; infection

J Nucl Med 2016; 57:67–69
DOI: 10.2967/jnumed.115.164020

System x_C^- is composed of xCT and 4F2hc, mediating cellular cystine uptake for glutathione synthesis to protect cells from oxidative stress (*1*). Several lines of evidence suggest that system x_C^- may play a role in the innate and adaptive immune system. Upregulation of system x_C^- expression was observed in activated macrophages and granulocytes (*2,3*). Induction of system x_C^- may be an autoprotective mechanism from the high levels of released reactive oxygen species (*4*). Activation of T-lymphocytes has been reported to involve expression of system x_C^- in antigen-presenting cells (*5,6*). Upregulation of xCT occurs during activation and differentiation of B lymphocyte (*7*). On the other hand, very low or no expression of xCT was detected in peripheral leukocytes, thymus, spleen, and lymph nodes in humans (*8*). These results suggest that system x_C^- is a key player in the active phase of inflammation.

(4*S*)-4-(3-^{18}F-fluoropropyl)-L-glutamate (^{18}F-FSPG) is a new L-glutamate derivative that is specifically taken up by system x_C^- as previously demonstrated in tumor models and cancer patients (*9,10*). Our primary objective was to explore ^{18}F-FSPG PET detection of inflammatory lesions of infectious or noninfectious cause. Secondary objectives were to perform quantitative analyses of ^{18}F-FSPG uptake and compare the results with those for ^{18}F-FDG. In addition, we evaluated the expression of xCT, CD44, and surface markers of inflammatory cells by immunohistochemistry to explore their correlation with ^{18}F-FSPG uptake.

MATERIALS AND METHODS

Study Design

The protocol of this open-label, nonrandomized, single-dose exploratory study was approved by both the Institutional Review Board and the Korea Food and Drug Administration. All patients provided written informed consent before participating.

Radiopharmaceutical Preparation

^{18}F-FSPG was radiolabeled as described previously (*9*). The specific activity of ^{18}F-FSPG formulated for intravenous administration was 74.4 ± 59.6 GBq/μmol (range, 35.0–235.6 GBq/μmol), and the radiochemical purity was 91.6% ± 1.5% (range, 90.1%–94.4%).

Patients

Patients were enrolled if they had inflammatory or infectious diseases with strong clinical or laboratory evidence of an inflammatory or infectious focus or foci in defined anatomic regions preferably visible on ^{18}F-FDG PET/CT scans. Full eligibility criteria are shown in Supplemental Appendix A (supplemental materials are available at http://jnm.snmjournals.org).

PET/CT Procedure

^{18}F-FDG and ^{18}F-FSPG PET/CT (*10*) was performed as previously described using the same PET/CT scanner (Biograph True Point 40; Siemens). ^{18}F-FSPG PET/CT was conducted during 3 time windows (0–45, 60–75, and 105–120 min) after injection of 300 ± 10 MBq of ^{18}F-FSPG.

Received Aug. 5, 2015; revision accepted Oct. 5, 2015.
For correspondence or reprints contact: Dae Hyuk Moon, Department of Nuclear Medicine, Asan Medical Center, University of Ulsan College of Medicine, 88, Olympic-ro 43-gil, Songpa-gu, Seoul 138-736, Korea.
E-mail: dhmoon@amc.seoul.kr
Published online Oct. 15, 2015.

Image Analysis

The PET/CT images were assessed visually and quantitatively by 2 board-certified nuclear medicine physicians as previously reported (*10*). SUV_{mean} was obtained to generate a time–activity profile of ^{18}F-FSPG uptake. The PET/CT images at 60 min after injection were used for visual and quantitative analysis. The largest inflammatory or infectious lesion was chosen as the representative lesion for patient-based analysis. As many as 5 of the largest lesions were selected as reference lesions. The SUV ratio was calculated by dividing the SUV_{max} of the reference lesion by the SUV_{mean} of blood-pool activity.

Immunohistochemical Staining of xCT, CD44, and Surface Markers of Inflammatory Cells

The immunohistochemical staining methods are shown in Supplemental Appendix A.

Statistical Analysis

Comparison was conducted using the Mann–Whitney *U* test, Fisher exact test, and Spearman rank correlation coefficients (ρ) on SPSS Statistics, version 21 (IBM), for Windows (Microsoft).

RESULTS

Patients and ^{18}F-FSPG PET/CT Procedure

Five men and 5 women were enrolled (age range, 42–66 y). All but 2 patients underwent ^{18}F-FDG PET/CT. The mean interval between ^{18}F-FDG and ^{18}F-FSPG PET/CT was 2.0 ± 1.8 d (range, 1–6 d). The baseline characteristics are summarized in Supplemental Table 1. Twenty-four reference lesions in 10 patients were selected (lung, 17; lymph node, 7).

Biodistribution of ^{18}F-FSPG

SUV_{mean} data for normal tissues and inflammatory or infectious lesions are summarized in Supplemental Figure 1. The kidney and pancreas showed high uptake, whereas the spleen exhibited low uptake. There was no or negligible uptake in the brain, myocardium, muscle, intestinal track, and bone.

^{18}F-FSPG Uptake in Inflammatory or Infectious Lesions

The patient-based (10/10, 7 major and 3 minor accumulations) and lesion-based (24/24, 15 major and 9 minor accumulations) detection rates by visual assessment were 100%.

All sarcoid reference lesions (10/10) showed major uptake (Fig. 1), whereas only 36% (5/14) of the nonsarcoid lesions had the same uptake (Supplemental Fig. 2, $P = 0.002$). SUV_{max} was significantly higher in sarcoidosis than in nonsarcoidosis, as was SUV ratio ($P < 0.001$, Fig. 2). SUV_{max} and SUV ratio for ^{18}F-FDG were also significantly higher in sarcoidosis than in nonsarcoidosis ($P = 0.001$ and 0.006, respectively, Fig. 2).

The visually assessed intensity of ^{18}F-FSPG accumulation in reference lesions was the same as that of ^{18}F-FDG (100%, 10/10) in sarcoidosis, whereas 92% (11/12) of the lesions in nonsarcoidosis had lower ^{18}F-FSPG accumulation (Supplemental Fig. 3). Quantitative analysis showed that SUV ratio for ^{18}F-FSPG in sarcoid lesions at 60 min after injection was comparable to that for ^{18}F-FDG ($P = 0.481$, Fig. 2A) although SUV_{max} was significantly lower for ^{18}F-FSPG than for ^{18}F-FDG ($P < 0.001$, Fig. 2B). In nonsarcoidosis, SUV_{max} and SUV ratio were significantly lower for ^{18}F-FSPG than for ^{18}F-FDG ($P < 0.05$, Fig. 2).

^{18}F-FSPG Uptake and Correlation with Immunohistochemical Staining

Eight patients underwent core-needle biopsy, but the tissue sample was sufficient from only 5 patients. The results of immunohistochemical analysis are shown in Supplemental Table 2. All 5 patients showed positive xCT expression in at least 50% of inflammatory cells. Histiocytes and plasma cells showed positive xCT staining (Fig. 1, Supplemental Figs. 2 and 4). In 2 of 3 patients with a major accumulation, the proportion of CD44 expression was at least 80% (Fig. 1 and Supplemental Fig. 4), whereas 2 patients with minor uptake showed no more than 30% positive cells (Supplemental Fig. 2). The proportion of immunohistochemical staining of xCT correlated significantly with that of CD68 ($\rho = 0.9$, $P = 0.037$). The SUV_{max} for ^{18}F-FSPG correlated negatively with CD163-positive cells, with borderline significance ($\rho = -0{,}872$, $P = 0.054$). However, no correlation was found with other surface markers of inflammatory cells.

DISCUSSION

We found that ^{18}F-FSPG uptake was significantly higher in patients with sarcoidosis than in patients with nonsarcoidosis. Inflammatory mechanisms of sarcoidosis include activation of macrophages and dendritic cells (*11*). Of note, 2 patients with sarcoidosis had elevated serum angiotensin-converting enzyme and systemic symptoms. On the other hand, patients with nonsarcoidosis presented with radiologic abnormalities without systemic symptoms. The inclusion of nonsarcoidosis patients was influenced by other diagnostic imaging studies that may have selected patients with a less active disease process and may have led to spectrum bias. This explanation is supported by higher ^{18}F-FDG uptake in patients with sarcoidosis than in patients with nonsarcoidosis.

The proportion of xCT-positive cells correlated significantly with that of CD68-positive cells. However, SUV_{max} for ^{18}F-FSPG did not correlate with xCT, CD44, or CD68 expression. The small number of patients and the limited amount of tissue available for immunohistochemical staining may have prevented us from obtaining a positive correlation. By contrast, previous examinations in tissue samples from tumor patients showed a correlation, suggesting that different or additional components contribute to uptake and retention in tumors

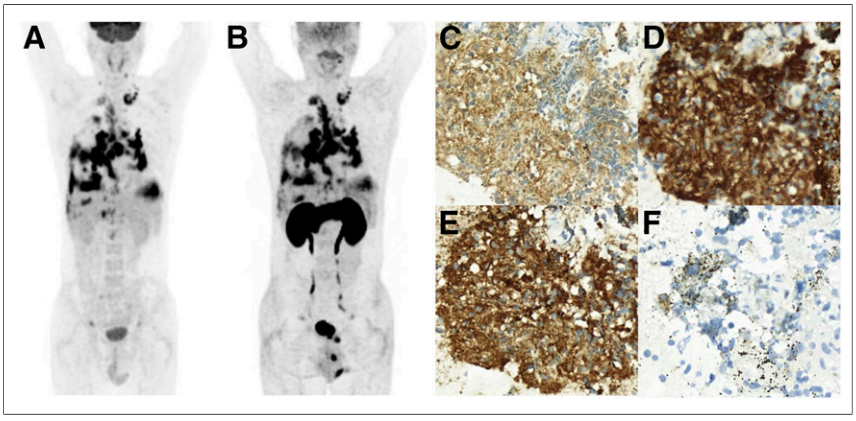

FIGURE 1. A 53-y-old man with sarcoidosis (patient 5). ^{18}F-FDG (A) and ^{18}F-FSPG (B) present similar major uptake involving pleura, supraclavicular lymph nodes, and thoracic lymph nodes. The only differences are normal physiologic uptake in brain, pancreas, and kidney. On immunohistochemistry evaluation (×400), proportion of inflammatory cells positive for xCT (C), CD44 (D), CD68 (E), and CD163 (F) was 80%, 80%, 80%, and 1%, respectively.

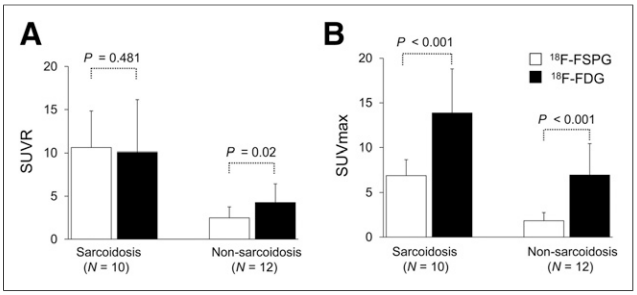

FIGURE 2. ^{18}F-FSPG and ^{18}F-FDG uptake in reference lesions at 60 min after injection. (A) SUV ratio (SUVR) did not significantly differ between ^{18}F-FSPG and ^{18}F-FDG in sarcoidosis but was significantly lower in nonsarcoidosis. (B) SUV_{max} for ^{18}F-FSPG was significantly lower than that for ^{18}F-FDG in both sarcoidosis and nonsarcoidosis.

and inflammatory tissue. The lack of correlation between ^{18}F-FSPG and xCT or CD44 may also result from the possibility that xCT expression has an additional role to play in remitting the chronic inflammatory response (*4*). In a mouse model of chronic inflammation induced by 3-methylcholanthrene, xCT messenger RNA was significantly upregulated, whereas xCT expression contributed to the termination of inflammation (*3,4*). In lipopolysaccharide-induced inflammation, a high initial rate of cystine uptake in macrophages was followed by a decrease in uptake at a later phase of inflammation (*2*). Finally, the regulation of CD44 on system x_C^- in inflammation may be different from that in cancer. There is a need for more studies on the regulation of system x_C^- activity in inflammation.

The SUV_{max} for ^{18}F-FSPG correlated negatively with CD163-positive staining, which is predominantly associated with M2 macrophages (*12*). Only 1% of cells showed positive CD163 staining in patient 5, who had sarcoidosis (Fig. 1), suggesting that most macrophages in this patient had the features of M1 macrophages. Our results may indicate that high ^{18}F-FSPG uptake represents an active disease state that is detectable by measuring xCT transporter activity in activated M1 macrophages. M1 and M2 macrophages appear to be oppositive, such as proinflammatory versus antiinflammatory (*13*). Our results suggest a potential usefulness of ^{18}F-FSPG PET in differentiating macrophage polarization. Our immunohistochemical results may also explain why ^{18}F-FSPG uptake was negligible 3 d after turpentine oil injection into the calf muscle (*9*).

The biodistribution of ^{18}F-FSPG here is consistent with previously reported data from cancer patients (*10*). The low background uptake would be especially advantageous in detecting inflammatory or infectious lesions in the brain, heart, and intestine, where the application of ^{18}F-FDG is limited because of normal physiologic uptake.

This study had several limitations. The detection rate must be considered with caution because of the small number of patients. Furthermore, most patients had pulmonary diseases. Immunohistochemical analysis was limited by the small amount of tissue available. Therefore, the current data are too limited to draw any firm conclusions from the immunohistochemical results.

CONCLUSION

^{18}F-FSPG PET may detect inflammatory lesions when activated macrophages or monocytes are present, such as in sarcoidosis. Further studies on a larger number of patients should be performed to validate whether ^{18}F-FSPG PET can detect foci in a greater variety of inflammatory or infectious diseases and from different body locations.

DISCLOSURE

The costs of publication of this article were defrayed in part by the payment of page charges. Therefore, and solely to indicate this fact, this article is hereby marked "advertisement" in accordance with 18 USC section 1734. This study was sponsored and financially supported by Bayer Pharma AG/Piramal Imaging GmbH, Berlin (Germany), and a Korea Health Technology R&D Project through the Korea Health Industry Development Institute (KHIDI), funded by the Ministry of Health and Welfare, Republic of Korea (HI06C0868). Drs. Oh and Moon received a research grant from Piramal Imaging GmbH. Drs. Koglin, Stephens, and Dinkelborg were employed by Piramal Imaging GmbH. Dr. Koglin has ownership interests in patents covering the applications of ^{18}F-FSPG. No other potential conflict of interest relevant to this article was reported.

REFERENCES

1. Lo M, Wang YZ, Gout PW. The x_c^- cystine/glutamate antiporter: a potential target for therapy of cancer and other diseases. *J Cell Physiol.* 2008;215:593–602.
2. Sato H, Fujiwara K, Sagara J, Bannai S. Induction of cystine transport activity in mouse peritoneal macrophages by bacterial lipopolysaccharide. *Biochem J.* 1995;310:547–551.
3. Nabeyama A, Kurita A, Asano K, et al. xCT deficiency accelerates chemically induced tumorigenesis. *Proc Natl Acad Sci USA.* 2010;107:6436–6441.
4. Lewerenz J, Hewett SJ, Huang Y, et al. The cystine/glutamate antiporter system x_c^- in health and disease: from molecular mechanisms to novel therapeutic opportunities. *Antioxid Redox Signal.* 2013;18:522–555.
5. Edinger AL, Thompson CB. Antigen-presenting cells control T cell proliferation by regulating amino acid availability. *Proc Natl Acad Sci USA.* 2002;99:1107–1109.
6. Angelini G, Gardella S, Ardy M, et al. Antigen-presenting dendritic cells provide the reducing extracellular microenvironment required for T lymphocyte activation. *Proc Natl Acad Sci USA.* 2002;99:1491–1496.
7. Vené R, Delfino L, Castellani P, et al. Redox remodeling allows and controls B-cell activation and differentiation. *Antioxid Redox Signal.* 2010;13:1145–1155.
8. Kim JY, Kanai Y, Chairoungdua A, et al. Human cystine/glutamate transporter: cDNA cloning and upregulation by oxidative stress in glioma cells. *Biochim Biophys Acta.* 2001;1512:335–344.
9. Koglin N, Mueller A, Berndt M, et al. Specific PET imaging of x_C^- transporter activity using a ^{18}F-labeled glutamate derivative reveals a dominant pathway in tumor metabolism. *Clin Cancer Res.* 2011;17:6000–6011.
10. Baek S, Choi CM, Ahn SH, et al. Exploratory clinical trial of (4S)-4-(3-[^{18}F]fluoropropyl)-L-glutamate for imaging x_C^- transporter using positron emission tomography in patients with non-small cell lung or breast cancer. *Clin Cancer Res.* 2012;18:5427–5437.
11. Valeyre D, Prasse A, Nunes H, Uzunhan Y, Brillet PY, Muller-Quernheim J. Sarcoidosis. *Lancet.* 2014;383:1155–1167.
12. Murray PJ, Allen JE, Biswas SK, et al. Macrophage activation and polarization: nomenclature and experimental guidelines. *Immunity.* 2014;41:14–20.
13. Stout RD, Suttles J. Functional plasticity of macrophages: reversible adaptation to changing microenvironments. *J Leukoc Biol.* 2004;76:509–513.